Erciyes Med J 2020; 42(3): 281–8 • DOI: 10.14744/etd.2020.61580
ORIGINAL ARTICLE – OPEN ACCESS

Diagnostic Efficacy of Signal Intensity Ratio and Apparent Diffusion Coefficient Measurements in Differentiating Cerebellopontine Angle Meningioma and Schwannoma

Mustafa Bozdağ[1], Ali Er[1], Sümeyye Ekmekçi[2]

ABSTRACT

Objective: To investigate the efficacy of Signal Intensity Ratio (SIR) measurements of T2-weighted imaging (T2WI) and Apparent Diffusion Coefficient (ADC) values of ADC mapping in the differentiation of schwannomas and meningiomas originating from the CPA.

Materials and Methods: A total of 30 patients who were pathologically diagnosed (16 meningiomas, 14 VS) were included in this retrospective study. SIR was calculated by proportioning regions of interests (ROIs) measurements of solid regions of the tumor and occipital subcutaneous adipose tissue in T2WI. In ADC maps, ADC_{min} and ADC_{mean} values were obtained by placing ROIs inside the solid parts of the tumor. Groups were statistically analyzed using the Mann-Whitney U test, independent-sample t-test, receiver operating characteristic (ROC) curve analyses, and Pearson correlation test.

Results: SIR, ADC_{mean}, and ADC_{min} values were 0.61±0.08, 0.858±0.101x10^{-3} mm^2/s, 0.815±0.099x10^{-3} mm^2/s for meningioma group; and 0.80±0.12, 1.272±0.148x10^{-3} mm^2/s, 1.232±0.148x10^{-3} mm^2/s for VS group, respectively. These parameters were statistically lower in the meningioma group compared to the VS group ($p<0.001$ for all). A positive correlation was observed between SIR and ADC values among the total group ($r=0.694$, $p<0.001$ for both). ROC analysis showed that the diagnostic performance of ADC parameters was better than the SIR parameter in differentiating meningioma from VS. The cut-off values in differentiating meningioma and VS were determined as 1.027x10^{-3} mm^2/s for ADC_{mean} and 0.980x10^{-3} mm^2/s for ADC_{min} with 100% sensitivity.

Conclusion: While both ADC and SIR values are useful in differentiating between VS and meningioma, ADC values have higher diagnostic efficacy compared to SIR.

Keywords: Apparent diffusion coefficient, signal intensity ratio, cerebellopontine angle, meningioma, schwannoma

Cite this article as:
Bozdağ M, Er A, Ekmekçi S. Diagnostic Efficacy of Signal Intensity Ratio and Apparent Diffusion Coefficient Measurements in Differentiating Cerebellopontine Angle Meningioma and Schwannoma. Erciyes Med J 2020; 42(3): 281-8.

[1]Department of Radiology, TR Ministry of Health İzmir Tepecik Training and Research Hospital, İzmir, Turkey
[2]Department of Pathology, TR Ministry of Health İzmir Tepecik Training and Research Hospital, İzmir, Turkey

Submitted
03.10.2019

Accepted
18.03.2020

Available Online Date
14.06.2020

Correspondence
Ali Er,
TR Ministry of Health İzmir Tepecik Training and Research Hospital, Department of Radiology, İzmir, Turkey
Phone: +90 212 404 15 00
e-mail: alier1717@yahoo.com

INTRODUCTION

Cerebellopontine angle (CPA) tumors constitute 6–10% of all cranial tumors (1). Vestibular schwannoma (VS) is the most common tumor to originate from this region (80–90%), followed by meningioma (5–10%) (2). Contrast-enhanced magnetic resonance imaging (MRI) is the gold standard imaging method in identifying CPA tumors. In most cases, CPA meningioma and schwannoma can be differentiated with conventional MRI; however, in some cases, imaging findings of these tumors may show significant overlapping in conventional MRI. Preoperational differentiation of these two tumors is essential and changes the treatment approach, especially surgical technique and prognosis. While the enlarged translabyrinthine approach is preferred in schwannomas, the retro-sigmoid approach is recommended in CPA meningiomas to preserve hearing function (3–5). CPA meningioma operations carry a lower risk of cranial nerve VII and VIII injury, though a higher rate of remission (6).

Schwannomas and meningiomas are generally hypo- or iso-intense in T1 weighted imaging (T1WI), whereas in T2 weighted imaging (T2WI), schwannomas generally show heterogeneous hyperintensity, and meningiomas show homogenous iso-intensity and hyperintense signal patterning (7, 8). Therefore, differences in signal intensity in T2WI may be useful in differentiating schwannomas from meningiomas. In addition to conventional MRI sequences, Diffusion-Weighted Imaging (DWI) also provides information on the histological and biological characteristics of brain tumors. In DWI, the contrast of the image is based on the motion of water molecules (9). High intratumoral cellularity obstructs the free motion of water molecules, referred to as restricted diffusion (10). The magnitude of restricted diffusion can be measured using Apparent Diffusion Coefficient (ADC) values from ADC maps. ADC values show a strong inverse correlation with tumoral cellularity (11). Previous studies have determined that ADC values are useful in differentiating various cerebral tumors, such as malignant from benign meningiomas, low from high-grade gliomas, high-grade gliomas from metastases (12–14). Recent studies also demonstrated many associations of ADC parameters estimated from the region of interest (ROI) and histogram-based methods with different histopathological features, such as the Ki-67 index, cellularity, cell count in several

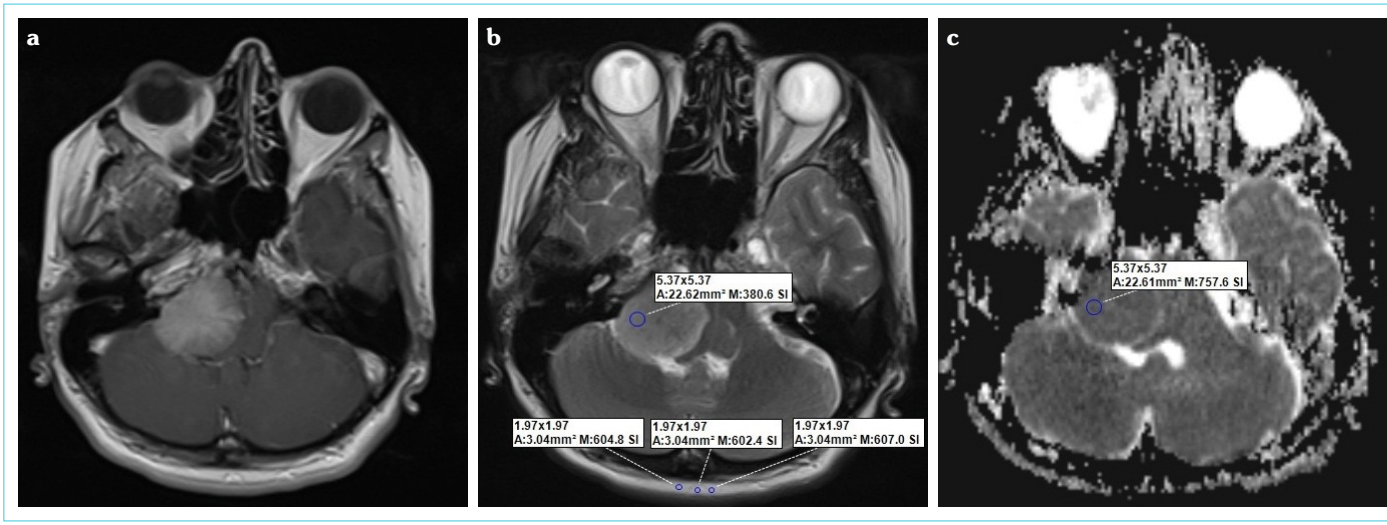

Figure 1. Example of image analysis. A contrast-enhancing solid mass is located on the right cerebellopontine angle (a). On the axial T2W image (b), ROIs are placed into the solid tumor and occipital subcutaneous fat. Signal intensity ratios of these lesions are calculated. On the ADC map (c), ROIs of the same size are carefully placed on the same regions corresponding to axial T2WI. ADC_{mean} and ADC_{min} values were calculated from these ROIs

tumors, including meningioma (15–18). There are few studies in the literature that have investigated the benefits of DWI in differentiating between schwannomas and meningiomas (19, 20).

Objectives

In our study, we investigated the efficacy of signal intensity ratio (SIR) on T2WI and ADC values in differentiating schwannomas and meningiomas of CPA origin.

MATERIALS and METHODS

Study Population

This retrospective study was approved by the Izmir Tepecik Training and Research Hospital Local Ethics Committee (approval date: 02.13.2019 issue number: 2019/2-13). We performed a radiology report database search in our hospital databases for the cases between November 2014 to January 2019 and found 185 patients reported to be "meningioma" (119 patients) or "schwannoma" (66 patients). In this study, we reviewed the images of 119 meningioma, 66 schwannoma cases. From schwannoma patients, 22 spinal cord, nine extremities, four trigeminal, one mandibular, and one parotid gland schwannoma cases were excluded from this study. The remaining 29 schwannoma tumors were originating from the CPA. Of the 119 meningioma cases, there were 24 meningioma cases that arise from the CPA. From 29 schwannoma and 24 meningioma cases, we excluded 17 patients who did not have a surgical invention, and we identified 36 patients who had undergone an MRI study before surgical intervention and had a pathological diagnosis of meningioma or schwannoma originating from the CPA. At last, we excluded six patients from this study. The exclusion criteria were as follows: (a) history of previous surgery or treatment of radiation therapy; (b) tumors smaller than 10 mm in diameter; (c) MRI without DWI study; (d) obvious motion artifacts on ADC maps which prevent accurate measurements. Finally, 14 schwannoma and 16 meningioma patients (16 female and 14 men) were enrolled in this study. The mean time interval between imaging and surgical invention was 9.8±10.3 days (range, 1–40 days) for meningioma cases and 21.5±14.7 days (range, 4–45 days) for schwannoma cases.

MRI Protocol

All brain MRI examinations of patients were performed using a 1.5 Tesla (T) scanner system (Aera, Siemens, Erlangen, Germany) using head coils. Patients underwent conventional MRI and DWI during the same procedure. DWI was obtained before the administration of the contrast medium. The conventional MR imaging protocol included: axial and sagittal T1W spin-echo (SE) sequence with repetition time (TR)/echo time (TE)=390/8.9ms, slice thickness (ST)=5 mm, field of view (FOV)=25 cm, and matrix size=240x320; axial and coronal T2W turbo spin-echo sequence (TSE) with TR/TE=5600/102 ms, ST=5 mm, FOV=25 cm, and matrix size=240x320; and axial fluid-attenuated inversion recovery (FLAIR) sequence with TR/TE=10370/82 ms and inversion time (IT)=2638. After intravenous administration of a single 0.1 mg/kg bolus dose of gadolinium, contrast-enhanced tri-planar T1W SE (TR/TE=390/8.9 ms) images were obtained. The DWI study was performed in the axial plane using a spin-echo, echo-planar imaging sequence with the following parameters: TR/TE=5600/115, FOV=230 mm, matrix size=192x192, slice thickness=5. DWI was performed with b values of 0 and 1000 s/mm^2. ADC maps were automatically reconstructed on a post-processing workstation.

Image Analysis

Conventional MR, DWI sequences were assessed by a radiologist (MB) who was blinded to the histopathological information of the patients. First, the tumor size was measured defined as the maximum diameter on contrast-enhanced T1WI. For quantitative signal analysis, SIR was calculated on the same image, defined as the signal intensity of the tumor divided by the signal intensity of the occipital subcutaneous fat as reference tissue (Fig. 1). The signal intensity of the tumor was measured using the average score from 5 ROI, which was obtained by manually positioning ROIs (10–40

Table 1. Demographic characteristics, maximum tumor size, ADC_{mean}, ADC_{min}, and SIR measurements for meningioma and schwannoma groups

Parameter	Meningioma group (n=16)	Schwannoma group (n=14)	p
Gender (F/M)	9/7	7/7	0.732[a]
Age (Year)	53	48	0.006[c]
Range	48–79	33–69	
Maximum tumor size (mm)	37.18±14.55	27.35±9.22	0.035[b]
Range	20–62	14–42	
ADC_{mean} ($x10^{-3}$ mm^2/s)	0.858±0.101	1.272±0.148	<0.001[b]
Range	0.707–1.027	0.983–1.485	
ADC_{min} ($x10^{-3}$ mm^2/s)	0.815±0.099	1.232±0.148	<0.001[b]
Range	0.684–0.980	0.944–1.423	
SIR	0.61±0.08	0.80±0.12	<0.001[b]
Range	0.47–0.74	0.54–0.98	

ADC: Apparent diffusion coefficient; SIR: Signal intensity ratio; F: Female; M: Male; mm: Millimeter. Values are given as mean values±SD for maximum tumor size, SIR, ADC_{min}, and ADC_{mean} parameters and as median values for patient age parameter; p: significance level for all pairs. a: Comparisons were performed using the Chi-square test; b: Comparisons were performed using the independent-sample t-test; c Comparisons were performed using the Mann-Whitney U test

mm^2) on T2W images inside the solid regions of the tumor. Solid regions of the tumor were determined as the enhanced area of the tumor corresponding to the contrast-enhanced-T1W sequence. The ROIs were placed strategically, avoiding hemorrhagic, cystic, and calcified regions using T2W and cranial CT images as reference. The signal intensity of the reference occipital subcutaneous adipose tissue was measured as the average of three ROIs of less than 5 mm^2 placed on the same axial T2W image slice. Signal intensity measurements were made by a radiologist (MB) who was blinded to the pathological data of the subjects.

For qualitative analysis of DWI, ADC measurements were performed using a Syngo workstation (Siemens, Erlangen, Germany). The ADC values were obtained by manually placing 5 uniform oval ROIs (10–40 mm^2) inside the solid parts of the tumor on the ADC maps in the same slice where SIR was measured (Fig. 1). Finally, the mean ADC (ADC_{mean}) values were calculated, and the lowest ADC value was chosen as the minimum ADC (ADC_{min}) from these ROIs. Careful attention was paid to obtain signal intensity and ADC measurements from the same areas of the tumor.

Statistical Analysis

Statistical analysis was performed using SPSS (Statistical Package for Social Sciences version 22.0, SPSS Inc., Chicago, Illinois, USA). Each parameter was calculated as the mean±standard deviation (SD). The normality of distribution of the parameters was assessed using the Shapiro-Wilk test. The Shapiro-Wilk test revealed that tumor diameter, SIR, ADC_{min}, and ADC_{mean} variables followed a normal distribution, and the patient age variable did not follow a normal distribution. Therefore, the statistically significant differences of maximum tumor diameter, SIR, ADC_{min}, and ADC_{mean} parameters between two independent groups were evaluated with the independent-sample t-test. The Mann-Whitney U test was used to explore the differences in patient age between two independent groups. In the relations between categorical variables, the chi-square test was applied. The correlation analysis between the SIR and ADC values was performed using Pearson's product-moment correlation. A value of $p<0.05$ was considered statistically significant. Receiver operating characteristic (ROC) analysis was used to determine a cut-off value to evaluate the diagnostic performance of the ADC_{min}, ADC_{mean}, and SIR values in differentiating CPA meningioma and schwannoma. Specificity, sensitivity, Youden index, and area under the curve (AUC) were calculated.

RESULTS

Among a total of 30 patients (16 female and 14 male), 14 patients were histologically diagnosed with schwannoma, and 16 patients with meningioma were included in this study. Of the meningioma cases, 14 were histologically Grade I (13 meningothelial, 1 fibrous) meningioma and 2 were Grade II. Demographic characteristics, tumor diameter, ADC_{min}, ADC_{mean}, and SIR values are summarized in Table 1. There was no significant difference between sexes among the two groups (p=0.732). The median age of the meningioma group was significantly higher compared to the schwannoma group (53 and 48, respectively; p=0.006). The maximum lesion size was significantly higher in the meningioma group compared to the schwannoma group (p=0.035). ADC_{mean}, ADC_{min}, and SIR values were significantly lower in CPA meningioma patients compared to schwannoma patients ($p<0.001$ for all). The comparison of ADC_{mean}, ADC_{min} and SIR values of the two groups is demonstrated in the box plot graph (Fig. 2).

ROC curve analyses of the differentiation of meningioma from schwannoma are demonstrated in Figure 3. ADC_{mean} and ADC_{min} were found to have better diagnostic efficacy in differentiating between schwannoma and meningioma compared to SIR parameters. The cut-off, AUC, Youden index, sensitivity, and specificity values of ADC_{mean}, ADC_{min} and SIR parameters are shown in Table 2. ADC_{mean} values were $<=1.027x10^{-3}$ mm^2/s and ADC_{min} values were $<=0.980x10^{-3}$ mm^2/s, in all meningioma patients. ADC values of VS patients were higher than that value except for one case. ADC_{mean}, and ADC_{min} values of that VS case were $0.983x10^{-3}$ mm^2/s and $0.944x10^{-3}$ mm^2/s, respectively (Fig. 4). There were

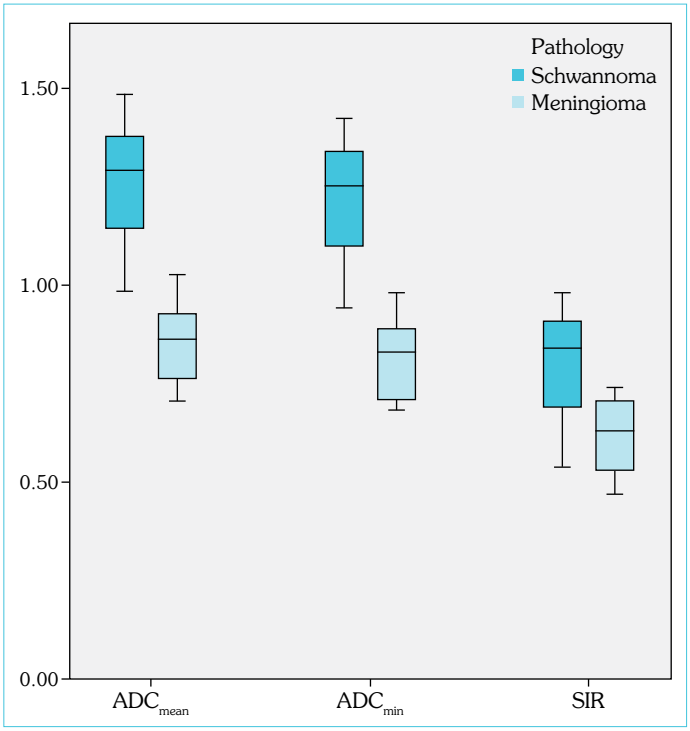

Figure 2. Box plot shows the comparison of ADC_{mean}, ADC_{min}, and SIR parameters between CPA meningioma and VS

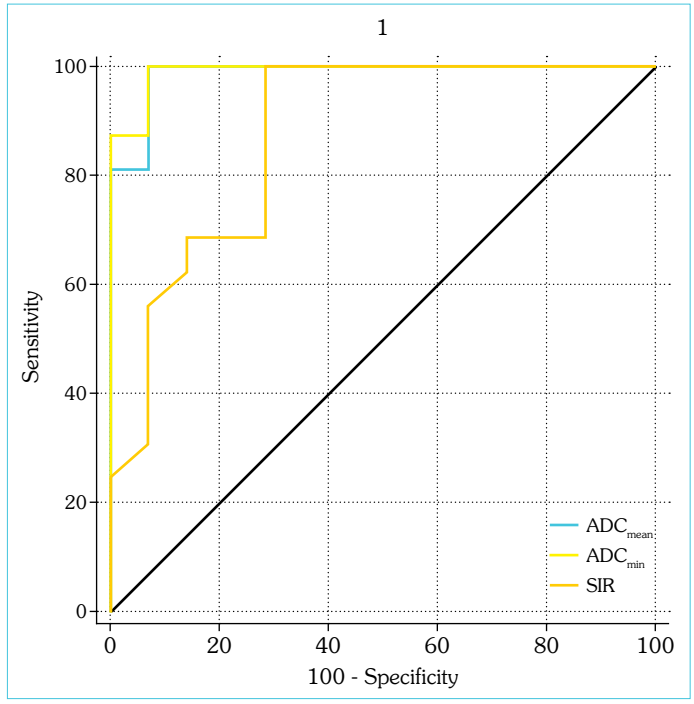

Figure 3. ROC analysis curves for ADCmean, ADCmin, and SIR parameters in differentiating CPA meningioma and VS. Area under the curve for ADC_{mean} is 0.987, ADC_{min} 0.991, SIR 0.875

Table 2. ROC results of ADC_{mean}, ADC_{min} and SIR parameters for differentiating VS and CPA meningioma

Parameter	AUC	Cut-off	Sensitivity	Specificity	Youden
ADC_{mean} (x10^{-3} mm^2/s)	0.987	1.027	92.86	100	92.86
ADC_{min} (x10^{-3} mm^2/s)	0.991	0.980	92.86	100	92.86
SIR	0.875	0.74	71.43	100	71.43

ROC: Receiver operating characteristic; ADC: Apparent diffusion coefficient; SIR: Signal intensity ratio; AUC: Area under the curve

significantly positive correlations between ADC_{mean} values and SIR values on T2WI (r=0.706, p<0.001) and ADC_{min} values and SIR values (r=0.711, p<0.001) in all patients included in this study (Fig. 5). Sample CPA meningioma and schwannoma cases are shown in Figure 6 and Figure 7, respectively.

DISCUSSION

The two most common extra-axial angle tumors of the CPA are the schwannoma (80–90%) and meningioma (5–10%). These two tumors differ in prognosis and treatment approaches. Thus, accurate preoperational diagnosis is important. With its high soft-tissue resolution and multiplanar evaluation capability, MRI is the preferred imaging method in evaluating CPA tumors. The benefits of imaging findings of computed tomography (CT) and MRI in radiologic differentiation between schwannoma and CPA meningioma have been previously described in detail (21). Findings of the broad dural base, eccentric placement to the internal auditory canal, and contrasting in adjacent dura known as dural tail support CPA meningioma, while elongation towards the internal auditory canal, central placement, and heterogenous contrasting are indicative of schwannoma (22–24). Overlapping of imaging features or lack of specific findings makes it difficult to distinguish between the two tumors. According to a previous study, approximately 25% of the CPA meningiomas are incorrectly diagnosed as schwannoma (25).

ADC values measured from ADC maps with DWI can be used to distinguish the two tumors. In our study, we investigated the efficacy of ADC_{mean} and ADC_{min} values in differentiating these two tumors. ADC_{mean} and ADC_{min} values were significantly lower in meningiomas compared to schwannomas (p<0.001 for both). Our results were similar to the findings obtained by Yamasaki et al. and Pavlisa et al. (19, 20). Both studies found that ADC_{mean} values significantly lower in CPA meningiomas compared to schwannomas. Other than that, few studies have investigated the utility of whole-tumor histogram analyses of ADC maps as a different technique in distinguishing VS from CPA meningioma and they reported that histogram analyses could also be useful in this differentiation (26, 27). Low intratumoral ADC values are related to high cellularity (11). Furthermore, ADC values derived from various measurement methods (predominantly histogram analysis based parameters) had shown their potential in reflecting many histopathological features in different tumors (17, 18, 28–31). Meningiomas have a relatively higher density of tumor cells and high nucleus/cytoplasm ra-

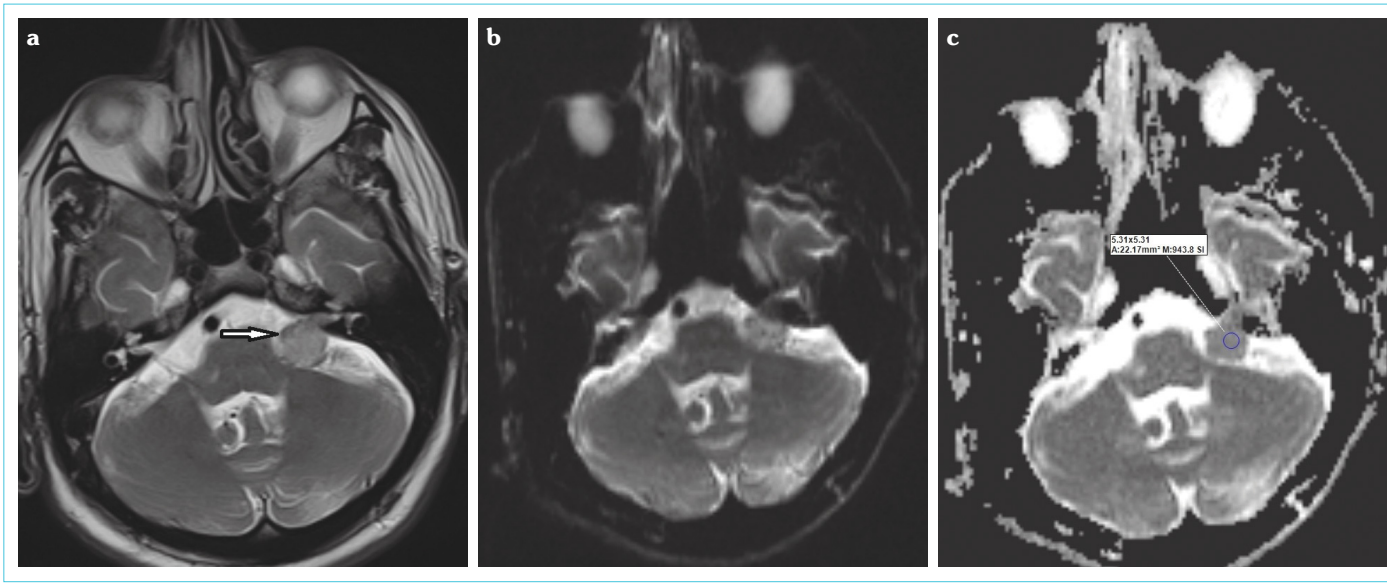

Figure 4. Representative images of a 50-year-old-man with left vestibular schwannoma (VS) shows mild-hyperintensity on axial T2WI (arrow) and a minimal extension of the lesion into the internal auditory canal (a). The lesion shows mild hyperintensity on the DWI map (b), isointensity on the ADC map (c) compared to the white matter of normal appearance and the calculated ADC (0.94x10^{-3} mm²/s) is lower than the optimum cut-off value

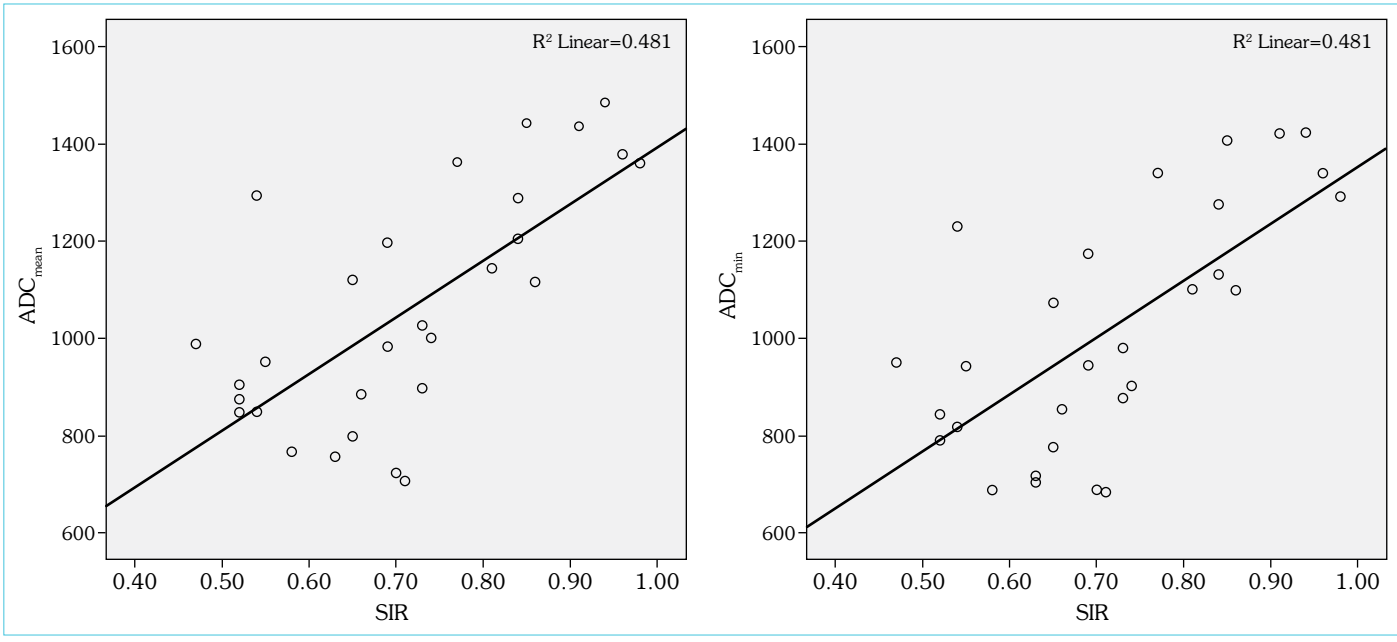

Figure 5. Correlation graphs between ADCmean and SIR, ADCmin and SIR values of all subjects

tio leading to restricted diffusion, in turn, is associated with low ADC values. In contrast, schwannomas are composed of both compactly organized cell regions (Antoni A) and loosely arranged hypocellular regions (Antoni B). Water diffusion occurs more easily in hypocellular Antoni B regions, which manifests as high ADC values. Although ADC measurements were made from solid regions outside of cystic-necrotic areas in conventional MRI, the presence of undeterminable intratumoral microcystic regions in MRI may have contributed to the relatively high ADC values.

SIR was calculated by measuring the ratio of mean tumoral signal intensity of CPA meningioma and schwannoma to the intensity of occipital subcutaneous adipose tissue in T2WI. To our knowledge, our study is the first study n the literature to use the SIR technique in differentiating between CPA meningioma and schwannoma. In our study, SIR values were significantly higher in CPA schwannomas compared to meningiomas ($p<0.001$). Schwannomas are generally more hyperintense and heterogeneous in T2WI compared to meningiomas. Small schwannomas are generally homogeneous and histologically consist of Antoni type A cells, and as they increase in size, they become more heterogeneous and increased ratio of Antoni Type B cells, leading to a cystic pattern (32). This yields the heterogeneous hyperintense appearance of schwannomas on T2WI. Meningiomas are generally homogeneous

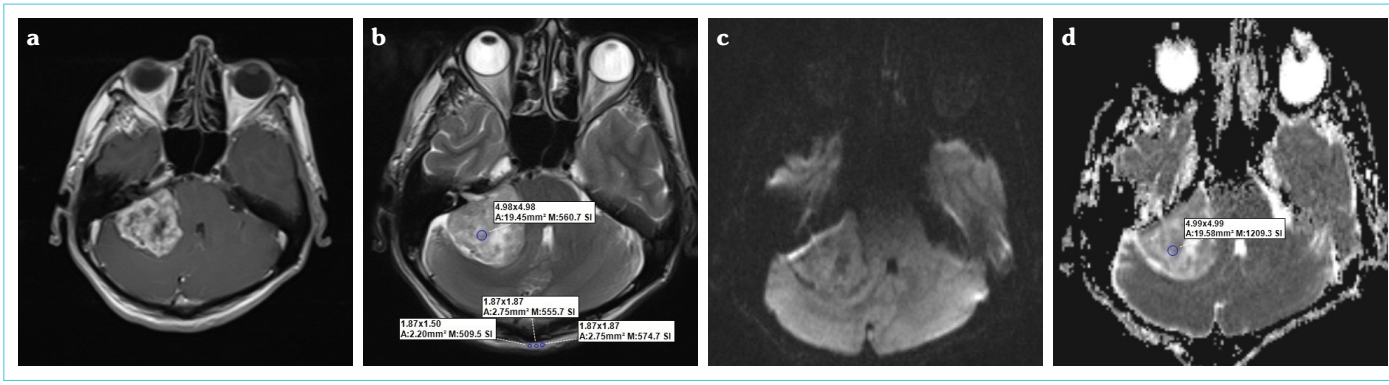

Figure 6. Representative images of a 45-year-old-man with right vestibular schwannoma (VS). Axial contrast-enhanced T1WI (a) demonstrates a heterogeneously enhanced mass located in the right CPA area without internal auditory canal involvement (arrow). Axial T2W image (b) shows heterogeneous iso-hyperintensity inside the mass. The solid areas of VS display isointensity on DWI (c) and mild-hyperintensity on the ADC map (d) compared to the white matter of normal appearance. Demonstrative signal intensity and ADC measurements with ROIs on axial T2WI (b) and the ADC map (d)

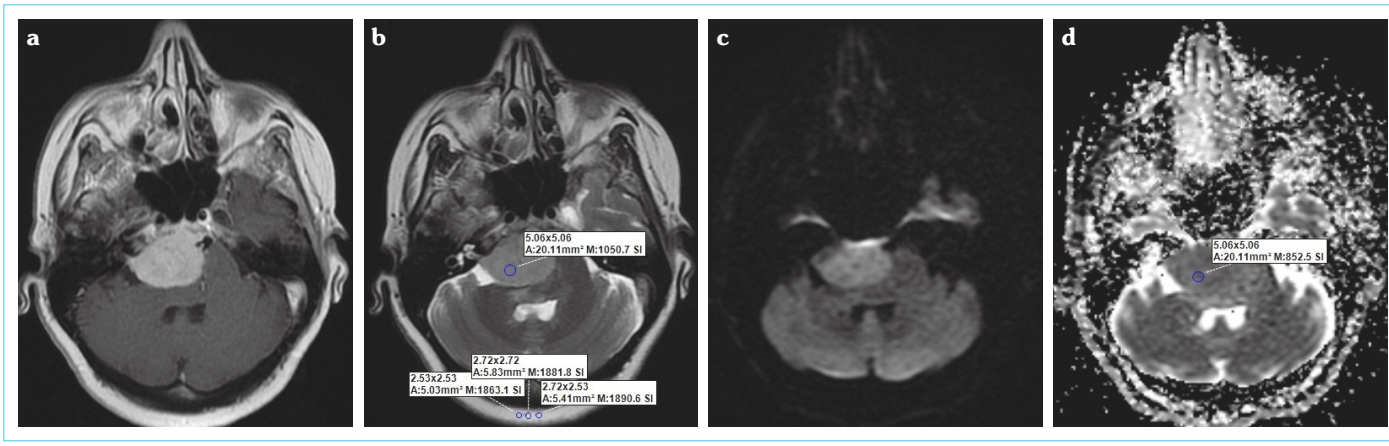

Figure 7. Representative images of a 53-year-old-man with right meningioma. A mass is located in the right cerebellopontine angle, showing homogeneous enhancement on axial contrast-enhanced T1WI (a) and mild-hyperintensity on axial T2WI (b). Note that contrast-enhanced T1WI (a) shows a minimal extension of the lesion into the internal auditory canal (arrow). The lesion shows mild hyperintensity on the DWI map (c) and isointensity on the ADC map (d) compared to the white matter of normal appearance. Demonstrative signal intensity and ADC measurements with ROIs on axial T2WI (b) and the ADC map (d)

on T2WI, and intratumoral cystic changes are rare and due to hemorrhage and aggressive nature (33). In our study, central cystic changes were seen in two patients with Grade II meningioma. As a result, our findings support that low ADC_{mean}, ADC_{min}, and SIR values support meningioma diagnosis, while high values support the diagnosis of schwannoma.

Since calcification may cause hypointensity in meningiomas, we measured signal intensity from contrasted solid regions outside of calcification using non-contrasted brain CT as a reference. In addition, we previously mentioned the presence of relatively higher cellularity in meningiomas. High cellularity may cause low ADC values along with decreased tumoral signal intensity on T2WI (32). Indeed, our study found a highly positive correlation between ADC_{mean}, ADC_{min}, and SIR values in meningiomas and schwannomas.

Retrospective analysis of our data showed distinct inconsistency in ADC (ADC_{mean}=1.027x10^{-3} mm^2/s, ADC_{min}=0.980x10^{-3} mm^2/s) and SIR (0.47) values in a case with pathological diagnosis of fibrous meningioma. High ADC values of histologically fibrous meningioma can be explained by its relatively low cellular density compared to other meningioma subtypes (34). Also, the more hypointense appearance on T2WI compared to the generally iso- mild hyperintensity, which arises from denser regions of the collagen matrix, manifests as lower SIR values (35).

According to ROC analyses, ADC values yielded better performance than SIR values in differentiating between the two tumors. Despite the clear overlapping in SIR values of both tumors, this was observed much less in ADC_{mean} and ADC_{min} values. Yamasaki et al. (19) compared ADC values in countless brain tumors and found prominent overlapping in ADC_{mean} values between meningiomas and schwannomas, which was inconsistent with our findings. However, in a newer study by Pavlisa et al. (20), which only included meningiomas and schwannoma tumors, there was no overlapping between ADC_{mean}, which was more consistent with our study. The meningioma group of Pavlisa et al.'s study was

also dominantly Grade I meningioma; however, there was no patient with Grade III meningioma in our study. Also, in our study, except for one patient, all of the Grade I meningioma patients was of meningothelial histological subtype, while Pavlisa et al.'s study did not mention histological subtype. We believe the narrow interval of ADC values of the meningioma group compared to the schwannoma group was due to the histological homogeneity of the meningioma patients. In a DWI study distinctly on the histological subtypes of meningioma, high ADC values (>1.00x10^{-3} mm^2/s) in addition to wide ADC intervals were noted in secretory, psammomatous, and transitional subtypes (36).

In our study, we determined the optimum cut-off values for ADC and SIR values for distinguishing the two tumors (Table 2). In the literature, Samadow et al. (37) defined an optimum cut-off value as 0.983x10^{-3} mm^2/s for ADC_{mean} with 100% sensitivity and 96.3% specificity, and the results were closer to our findings, but the study sample size was low as in our study. Other authors did not define a threshold value in their studies (19, 20). We think that further studies with a higher number of cases are warranted to define a threshold value. In our study, we found ADC values of all meningioma patients were lower than or equal to cut-off values. ADC value of only one VS case was lower than the cut-off values. The tumor size of this case (17 mm) was relatively smaller than other VS cases (Fig. 4). As mentioned before, small schwannomas are generally composed of Antoni A cell areas that exhibit a more compactly packed architecture and less microcystic areas, resulting in relatively low ADC values. Furthermore, intratumoral microhemorrhages are frequently seen in VS, and sometimes only appear as susceptibility signals on susceptibility-weighted imaging (SWI) or T2 * gradient-echo sequences (38). These microhemorrhages may be another reason for measuring lower ADC values in this case.

Our study had some limitations. First, the design of our study was retrospective. Secondly, the patient sample size was small. In addition, as mentioned above, except for three patients in the meningioma group (2 atypical meningiomas, 1 fibrous meningioma), all other patients constituted a single pathological group. There is a need for further studies with a larger patient population, more pathological subtypes, including Grade III (anaplastic) meningioma, comparing schwannoma and meningioma patient groups. Secondly, tiny intratumoral hemorrhages, which can be identified SWI or T2* gradient-echo sequences, but indistinguishable in conventional MRI sequences, that mostly occur in schwannomas, may have affected our ROI measurements. Further studies involving SWI or T2* gradient-echo sequences could be planned for the future. Last, only ADC_{min}, ADC_{mean} and SIR were obtained by manually drawing ROIs on several solid parts of the tumor. However, tumor heterogeneity and tissue characteristics of the whole tumor can be quantified more comprehensively by whole lesion and histogram-based approaches compared to ROI measurement methods.

CONCLUSION

In conclusion, SIR on T2WI and ADC_{mean} and ADC_{min} values from ADC maps were significantly lower in CPA meningiomas compared to schwannomas. While both ADC and SIR values are useful in differentiating between these two tumors, ADC values hold higher diagnostic efficacy compared to SIR.

Ethics Committee Approval: This retrospective study was approved by the İzmir Tepecik Training and Research Hospital Local Ethics Committee (approval date: 02.13.2019 issue number: 2019/2-13).

Informed Consent: Written informed consent was obtained from patients who participated in this study.

Peer-review: Externally peer-reviewed.

Author Contributions: Concept – MB, AE; Design – MB, AE; Supervision – MB, AE; Resource – MB; Materials – MB, SE; Data Collection and/or Processing – AE, SE; Analysis and/or Interpretation – MB, AE, SE; Literature Search – MB, AE; Writing – MB; Critical Reviews – AE, SE.

Conflict of Interest: The authors have no conflict of interest to declare.

Financial Disclosure: The authors declared that this study has received no financial support.

REFERENCES

1. Nakamura M, Roser F, Dormiani M, Matthies C, Vorkapic P, Samii M. Facial and cochlear nerve function after surgery of cerebellopontine angle meningiomas. Neurosurgery 2005; 57(1): 77–90. [CrossRef]
2. Chen AF, Samy RN, Gantz BJ. Cerebellopontine angle tumor composed of Schwann and meningeal proliferations. Arch Otolaryngol Head Neck Surg 2001; 127(11): 1385–9. [CrossRef]
3. Robertson JT, Coakham HB, Robertson JH. Nerve Sheath Tumors. Chapter 27. Cranial Base Surgery. Churchill Livingstone; 2000.p.485–501.
4. Martuza RL, Ojemann RG. Bilateral acoustic neuromas: clinical aspects, pathogenesis, and treatment. Neurosurgery 1982; 10(1): 1–12.
5. Samii M, Matthies C. Management of 1000 vestibular schwannomas (acoustic neuromas): surgical management and results with an emphasis on complications and how to avoid them. Neurosurgery 1997; 40(1): 11–23. [CrossRef]
6. Mallucci CL, Ward V, Carney AS, O'Donoghue GM, Robertson I. Clinical features and outcomes in patients with non-acoustic cerebellopontine angle tumours. J Neurol Neurosurg Psychiatry 1999; 66(6): 768–71. [CrossRef]
7. Skolnik AD, Loevner LA, Sampathu DM, Newman JG, Lee JY, Bagley LJ, et al. Cranial Nerve Schwannomas: Diagnostic Imaging Approach. Radiographics 2016; 36(5): 1463–77. [CrossRef]
8. Watts J, Box G, Galvin A, Brotchie P, Trost N, Sutherland T. Magnetic resonance imaging of meningiomas: a pictorial review. Insights Imaging 2014; 5(1): 113–22. [CrossRef]
9. Chilla GS, Tan CH, Xu C, Poh CL. Diffusion weighted magnetic resonance imaging and its recent trend-a survey. Quant Imaging Med Surg 2015; 5(3): 407–22.
10. Koh DM, Collins DJ. Diffusion-weighted MRI in the body: applications and challenges in oncology. AJR Am J Roentgenol 2007; 188(6): 1622–35. [CrossRef]
11. Chen L, Liu M, Bao J, Xia Y, Zhang J, Zhang L, et al. The correlation between apparent diffusion coefficient and tumor cellularity in patients: a meta-analysis. PLoS One 2013; 8(11): e79008. [CrossRef]
12. Surov A, Ginat DT, Sanverdi E, Lim CCT, Hakyemez B, Yogi A, et al. Use of diffusion weighted imaging in differentiating between malignant and benign meningiomas. A multicenter analysis. World Neurosurg 2016; 88: 598–602. [CrossRef]
13. Kono K, Inoue Y, Nakayama K, Shakudo M, Morino M, Ohata K, et al. The role of diffusion-weighted imaging in patients with brain tumors. AJNR Am J Neuroradiol 2001; 22(6): 1081–8.
14. Lee EJ, terBrugge K, Mikulis D, Choi DS, Bae JM, Lee SK, et al. Diagnostic value of peritumoral minimum apparent diffusion coefficient

for differentiation of glioblastoma multiforme from solitary metastatic lesions. AJR Am J Roentgenol 2011; 196(1): 71–6. [CrossRef]
15. Surov A, Gottschling S, Mawrin C, Prell J, Spielmann RP, Wienke A, et al. Diffusion-Weighted Imaging in Meningioma: Prediction of Tumor Grade and Association with Histopathological Parameters. Transl Oncol 2015; 8(6): 517–23. [CrossRef]
16. Surov A, Hamerla G, Meyer HJ, Winter K, Schob S, Fiedler E. Whole lesion histogram analysis of meningiomas derived from ADC values. Correlation with several cellularity parameters, proliferation index KI 67, nucleic content, and membrane permeability. Magn Reson Imaging 2018; 51: 158–62. [CrossRef]
17. Surov A, Meyer HJ, Wienke A. Correlation between apparent diffusion coefficient (ADC) and cellularity is different in several tumors: a meta-analysis. Oncotarget 2017; 8(35): 59492–9. [CrossRef]
18. Surov A, Meyer HJ, Wienke A. Associations between apparent diffusion coefficient (ADC) and KI 67 in different tumors: a meta-analysis. Part 1: ADCmean. Oncotarget 2017; 8(43): 75434–44. [CrossRef]
19. Yamasaki F, Kurisu K, Satoh K, Arita K, Sugiyama K, Ohtaki M, et al. Apparent diffusion coefficient of human brain tumors at MR imaging. Radiology 2005; 235(3): 985–91. [CrossRef]
20. Pavlisa G, Rados M, Pazanin L, Padovan RS, Ozretic D, Pavlisa G. Characteristics of typical and atypical meningiomas on ADC maps with respect to schwannomas. Clin Imaging 2008; 32(1): 22–7. [CrossRef]
21. Lalwani AK, Jackler RK. Preoperative differentiation between meningioma of the cerebellopontine angle and acoustic neuroma using MRI. Otolaryngol Head Neck Surg 1993; 109(1): 88–95. [CrossRef]
22. Bonneville F, Savatovsky J, Chiras J. Imaging of cerebellopontine angle lesions: an update. Part 1: enhancing extra-axial lesions. Eur Radiol 2007; 17(10): 2472–82. [CrossRef]
23. Le Garlantezec C, Vidal VF, Guerin J, Bébéar JP, Liguoro D, Darrouzet V. Management of cerebellopontine angle meningiomas and the posterior part of the temporal bone. Report on 44 cases.[Article in French]. Rev Laryngol Otol Rhinol 2005; 126(2): 81–9.
24. Guermazi A, Lafitte F, Miaux Y, Adem C, Bonneville JF, Chiras J. The dural tail sign--beyond meningioma. Clin Radiol 2005; 60(2): 171–88.
25. Grey PL, Moffat DA, Hardy DG. Surgical results in unusual cerebellopontine angle tumours. Clin Otolaryngol Allied Sci 1996; 21(3): 237–43. [CrossRef]
26. Xu XQ, Li Y, Hong XN, Wu FY, Shi HB. Radiological indeterminate vestibular schwannoma and meningioma in cerebellopontine angle area: differentiating using whole-tumor histogram analysis of apparent diffusion coefficient. Int J Neurosci 2017; 127(2): 183–90. [CrossRef]
27. Nagano H, Sakai K, Tazoe J, Yasuike M, Akazawa K, Yamada K. Whole-tumor histogram analysis of DWI and QSI for differentiating between meningioma and schwannoma: a pilot study. Jpn J Radiol 2019; 37(10): 694–700. [CrossRef]
28. Schob S, Meyer J, Gawlitza M, Frydrychowicz C, Müller W, Preuss M, Bure L, et al. Diffusion-Weighted MRI Reflects Proliferative Activity in Primary CNS Lymphoma. PLoS One 2016; 11(8): e0161386. [CrossRef]
29. Meyer HJ, Höhn A, Surov A. Histogram analysis of ADC in rectal cancer: associations with different histopathological findings including expression of EGFR, Hif1-alpha, VEGF, p53, PD1, and KI 67. A preliminary study. Oncotarget 2018; 9(26): 18510–7. [CrossRef]
30. Schob S, Voigt P, Bure L, Meyer HJ, Wickenhauser C, Behrmann C, et al. Diffusion-Weighted Imaging Using a Readout-Segmented, Multishot EPI Sequence at 3 T Distinguishes between Morphologically Differentiated and Undifferentiated Subtypes of Thyroid Carcinoma-A Preliminary Study. Transl Oncol 2016; 9(5): 403–10. [CrossRef]
31. Meyer HJ, Gundermann P, Höhn AK, Hamerla G, Surov A. Associations between whole tumor histogram analysis parameters derived from ADC maps and expression of EGFR, VEGF, Hif 1-alpha, Her-2 and Histone 3 in uterine cervical cancer. Magn Reson Imaging 2019; 57: 68–74. [CrossRef]
32. Gomez-Brouchet A, Delisle MB, Cognard C, Bonafe A, Charlet JP, Deguine O, et al. Vestibular schwannomas: correlations between magnetic resonance imaging and histopathologic appearance. Otol Neurotol 2001; 22(1): 79–86. [CrossRef]
33. Go KO, Lee K, Heo W, Lee YS, Park YS, Kim SK, et al. Cystic Meningiomas: Correlation between Radiologic and Histopathologic Features. Brain Tumor Res Treat 2018; 6(1): 13–21. [CrossRef]
34. Maiuri F, Iaconetta G, de Divitiis O, Cirillo S, Di Salle F, De Caro ML. Intracranial meningiomas: correlations between MR imaging and histology. Eur J Radiol 1999; 31(1): 69–75. [CrossRef]
35. Soyama N, Kuratsu J, Ushio Y. Correlation between magnetic resonance images and histology in meningiomas: T2-weighted images indicate collagen contents in tissues. Neurol Med Chir (Tokyo) 1995; 35(7): 438–41. [CrossRef]
36. Sanverdi SE, Ozgen B, Oguz KK, Mut M, Dolgun A, Soylemezoglu F, et al. Is diffusion-weighted imaging useful in grading and differentiating histopathological subtypes of meningiomas? Eur J Radiol 2012; 81(9): 2389–95. [CrossRef]
37. Samadov P, Gündoğmuş CA, Ekinci G. Can we use diffusion weighted-MRI to differentiate cerebellopontine angle meningioma and vestibular schwannoma. Poster C-1129 presented at: the European Society of Radiology Meeting(EPOS); 2017 March 1-5; Vienna, Austria.
38. Mishra A, Thomas B, Kapilamoorthy TR. Susceptibility weighted imaging - a problem-solving tool in differentiation of cerebellopontine angle schwannomas and meningiomas. Neuroradiol J 2017; 30(3): 253–8.